

PACS 78.40.Ha, 77.80.Bh

## Electrical and optical parameters of $\text{Cu}_6\text{PS}_5\text{I}$ -based thin films deposited using magnetron sputtering

I.P. Studenyak<sup>1</sup>, A.V. Bendak<sup>1</sup>, V.Yu. Izai<sup>1</sup>, P.P. Guranich<sup>1</sup>, P. Kúš<sup>2</sup>, M. Mikula<sup>2</sup>, B. Grančič<sup>2</sup>, M. Zahoran<sup>2</sup>, J. Greguš<sup>2</sup>, A. Vincze<sup>2</sup>, T. Roch<sup>2</sup>, T. Plecenik<sup>2</sup>

<sup>1</sup>*Uzhhorod National University, Faculty of Physics,  
3, Narodna Sq., 88000 Uzhhorod, Ukraine*

<sup>2</sup>*Comenius University, Faculty of Mathematics, Physics and Informatics,  
Mlynska dolina, 84248 Bratislava, Slovakia,  
E-mail: studenyak@dr.com*

**Abstract.**  $\text{Cu}_6\text{PS}_5\text{I}$ -based thin films were deposited onto silicate glass substrates by non-reactive radio-frequency magnetron sputtering. The chemical composition of thin films was determined using energy-dispersive X-ray spectroscopy. Electrical conductivity of  $\text{Cu}_6\text{PS}_5\text{I}$ -based thin films was studied as dependent on chemical composition. Optical transmission spectra of  $\text{Cu}_{5.46}\text{P}_{1.68}\text{S}_{5.06}\text{I}_{0.80}$  thin film were investigated within the temperature interval 77...300 K; temperature behaviour of optical absorption spectra and dispersion of the refractive index were also studied. Temperature dependences of the energy position of absorption edge, Urbach energy and refractive index of  $\text{Cu}_{5.46}\text{P}_{1.68}\text{S}_{5.06}\text{I}_{0.80}$  thin film have been analyzed.

**Keywords:** thin film, magnetron sputtering, electrical conductivity, optical absorption, refractive index.

Manuscript received 15.12.15; revised version received 03.02.16; accepted for publication 16.03.16; published online 08.04.16.

### 1. Introduction

$\text{Cu}_6\text{PS}_5\text{I}$  crystalline chalcogenides belong to the superionic conductors with argyrodite structure. They are the promising materials for wide application as the solid electrolytes, fuel cells, ion-selective membranes, gas sensors and other electrochemical devices. Development and investigation of new technological superionic conductors with high operation parameters are important tasks for modern energetics that puts in the forefront the problems of the non-traditional energy sources construction.

$\text{Cu}_6\text{PS}_5\text{I}$  superionic conductors belong to the argyrodite family, and are characterized by high ionic conductivity, and due to this they are prospective

materials for creating renewable energy sources, electrochemical and optical sensors [1-4]. At room temperature, they belong to the cubic syngony  $F\bar{4}3m$ . With temperature decrease, two phase transitions occur, first of them at  $T_{II} = (269 \pm 2)$  K is the structural second-order phase transition (accompanied by the change of symmetry  $F\bar{4}3m \rightarrow F\bar{4}3c$ ), and the second – at  $T_I = (144 \pm 1)$  K is at the same time superionic and ferroelastic first-order phase transition (accompanied by the change of symmetry  $F\bar{4}3c \rightarrow Cc$ ) [5].

Optical absorption, luminescence, Raman scattering, refractive index dispersion for  $\text{Cu}_6\text{PS}_5\text{I}$  crystals were extensively studied in the works [6-8]. It should be noted that, at low temperatures, at the optical absorption edge the exciton bands are observed, which

with temperature increase become broader and are entirely smeared at the transition to the superionic state. In the superionic phase, the optical absorption edge has an exponential form, and his temperature behaviour can be described using the Urbach rule [7]. It is shown [7] that Urbach behaviour of the absorption edge is caused by exciton-phonon interaction, and its additional smearing is caused by the temperature-related and structural disordering; the latter in superionic conductors consists of static and dynamic components.

At the same time the optical properties of  $\text{Cu}_6\text{PS}_5\text{I}$  single crystals are well known, while investigation of physical properties of thin films on their basis only begins. It should be noted that the thin films based on superionic conductors can be applied to the production of supercapacitors of new generation [9]. In comparison to the traditional type of capacitors, they are characterized by small dimensions and high capacitances. The above mentioned advantages make this type of capacitors actual for development and preparation of autonomous nano- and microsystems as well as the powerful energy sources.

It should be noted that  $\text{Cu}_6\text{PS}_5\text{I}$  thin films were for the first time obtained and studied in Ref. [10]. Structural investigations show the films to be amorphous and have homogeneous two-dimensional structure. Isoabsorption studies reveal that at  $T = 470$  K the  $\text{Cu}_6\text{PS}_5\text{I}$  film is partially destructed and detached from the substrate. The influence of annealing on optical absorption edge parameters of  $\text{Cu}_6\text{PS}_5\text{I}$  thin films was investigated in Ref. [11].

In this paper, we report on deposition of  $\text{Cu}_6\text{PS}_5\text{I}$ -based thin films by non-reactive radio-frequency magnetron sputtering, investigation of electrical conductivity as well as temperature studies of optical absorption edge, investigations of temperature behaviour of the energy position of absorption edge, Urbach energy and refractive index.

## 2. Experimental

For synthesis of  $\text{Cu}_6\text{PS}_5\text{I}$  compounds, Cu, S, P, CuI in accordance with the stoichiometric ratio were placed into an evacuated silica ampoule. The ampoule was heated with the rate 100 K/h to the temperature 450...500 K and kept at this temperature for 24 h. Then, with the rate 100 K/h the temperature was increased to the maximal value 1020...1070 K, and the ampoule was kept at this temperature for 5 to 6 days, then they it was down to room temperature with the rate 100 K/h. The microcrystalline powder with the average grain size of 50  $\mu\text{m}$  was obtained by grinding of the synthesized material in an agate mortar.

$\text{Cu}_6\text{PS}_5\text{I}$ -based thin films were deposited onto silicate glass substrates by using non-reactive radio frequency magnetron sputtering; the film growth rate was close to 3 nm/min. The deposition was carried out at room temperature in Ar atmosphere. Structural

properties of the thin films under investigation were studied using SEM (Hitachi S-4300). Energy-dispersive X-ray spectroscopy (EDX) was used to ensure the thin films chemical composition (Table 1). With the increase of copper content, the increase of halogen content and decrease of phosphorous and sulphur were observed.

Electrical conductivity was measured by impedance meter at the frequency 1 MHz. Optical transmission spectra of  $\text{Cu}_6\text{PS}_5\text{I}$ -based thin films were studied in the interval of temperatures 77...300 K by using the MDR-3 grating monochromator, UTREX cryostat was used for low-temperature studies. Spectral dependences of absorption coefficient and dispersion dependences of refractive index of thin films were calculated on their basis.

## 3. Results and discussion

Electrical studies have shown that the total electric conductivity of the thin films increases with increasing the content of Cu atoms. Thus, with the Cu content increase in the interval from  $\text{Cu}_{5.37}\text{P}_{1.88}\text{S}_{5.04}\text{I}_{0.71}$  to  $\text{Cu}_{7.55}\text{P}_{0.89}\text{S}_{3.44}\text{I}_{1.12}$  the electric conductivity increases from 0.044 to 0.066 S/m. It should be noted that the total electrical conductivity for the  $\text{Cu}_6\text{PS}_5\text{I}$  single crystal is  $\sigma_t = 0.13$  S/m at 1 kHz [6]. The high value of electrical conductivity in thin films under investigation makes them promising materials for creation of solid state batteries and supercapacitors.

Futhermore, with the Cu content increase, a red shift of the optical transmission spectra as well as absorption edge spectra is observed. Temperature variations of optical transmission in  $\text{Cu}_6\text{PS}_5\text{I}$ -based thin films are similar for all the investigated samples (Table 1), but we will illustrate it for  $\text{Cu}_{5.46}\text{P}_{1.68}\text{S}_{5.06}\text{I}_{0.80}$  thin film. Thus, interferential transmission spectra of  $\text{Cu}_{5.46}\text{P}_{1.68}\text{S}_{5.06}\text{I}_{0.80}$  thin film at various temperatures within the range 77...300 K are shown in Fig. 1. With the temperature increase, a red shift of both the short-wave part of the transmission spectrum (related to the temperature behaviour of the absorption edge) and the interferential maxima is observed. Besides, a typical decrease of transmission in the interferential maxima with temperature is revealed.

**Table 1. Chemical content and electrical conductivity for  $\text{Cu}_6\text{PS}_5\text{I}$ -based thin films.**

Films	Chemical content	Electrical conductivity, $\sigma$ (S/m)
1	$\text{Cu}_{5.37}\text{P}_{1.88}\text{S}_{5.04}\text{I}_{0.71}$	0.044
2	$\text{Cu}_{5.46}\text{P}_{1.68}\text{S}_{5.06}\text{I}_{0.80}$	0.047
3	$\text{Cu}_{5.56}\text{P}_{1.66}\text{S}_{4.93}\text{I}_{0.85}$	0.049
4	$\text{Cu}_{5.70}\text{P}_{1.61}\text{S}_{4.74}\text{I}_{0.95}$	0.051
5	$\text{Cu}_{6.77}\text{P}_{1.12}\text{S}_{3.98}\text{I}_{1.14}$	0.056
6	$\text{Cu}_{7.55}\text{P}_{0.89}\text{S}_{3.44}\text{I}_{1.12}$	0.066

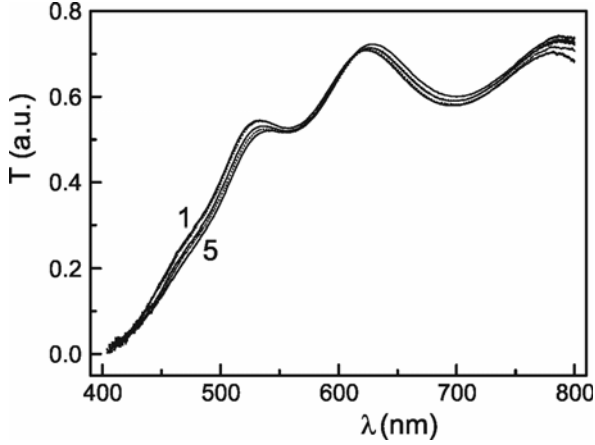


**Fig. 1.** Optical transmission spectra of  $\text{Cu}_{5.46}\text{P}_{1.68}\text{S}_{5.06}\text{I}_{0.80}$  thin film at various temperatures: 77 (1), 150 (2), 200 (3), 250 (4), and 300 (5) K.

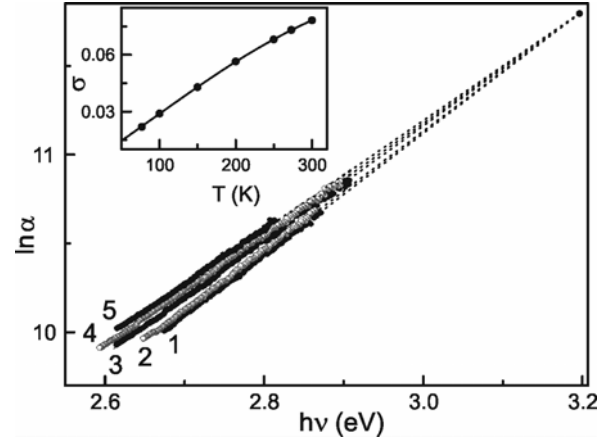


**Fig. 2.** Spectral dependences of the absorption coefficient of  $\text{Cu}_{5.46}\text{P}_{1.68}\text{S}_{5.06}\text{I}_{0.80}$  thin film at various temperatures: 77 (1), 150 (2), 200 (3), 250 (4), and 300 (5) K. The insert shows the temperature dependence of the steepness parameter  $\sigma$ .

It is seen (Fig. 2) that the optical absorption edge spectra within the range of their exponential behaviour in  $\text{Cu}_{5.46}\text{P}_{1.68}\text{S}_{5.06}\text{I}_{0.80}$  thin film are described by the Urbach rule [12]

$$\alpha(h\nu, T) = \alpha_o \cdot \exp\left[\frac{\sigma(h\nu - E_0)}{kT}\right] = \alpha_o \cdot \exp\left[\frac{h\nu - E_0}{E_U(T)}\right], \quad (1)$$

where  $E_U$  is the Urbach energy (a reciprocal of the absorption edge slope  $E_U^{-1} = \Delta(\ln\alpha)/\Delta(h\nu)$ ),  $\sigma$  is the absorption edge steepness parameter,  $\alpha_o$  and  $E_0$  are the convergence point coordinates of the Urbach bundle. The coordinates of the Urbach bundle convergence point  $\alpha_o$  and  $E_0$  for the  $\text{Cu}_{5.46}\text{P}_{1.68}\text{S}_{5.06}\text{I}_{0.80}$  thin film are given in Table 2.

**Table 2.** Parameters of Urbach absorption edge and EPI for  $\text{Cu}_{5.46}\text{P}_{1.68}\text{S}_{5.06}\text{I}_{0.80}$  thin film.

Film	$\text{Cu}_{5.46}\text{P}_{1.68}\text{S}_{5.06}\text{I}_{0.80}$
$\alpha_o$ ( $\text{cm}^{-1}$ )	$1.32 \cdot 10^5$
$E_0$ (eV)	3.197
$E_g^\alpha$ (eV)	2.876
$E_U$ (meV)	332
$\sigma_0$	0.131
$\hbar\omega_p$ (meV)	78.2
$\theta_E$ (K)	907
$(E_U)_0$ (meV)	299
$(E_U)_1$ (meV)	652
$E_g^\alpha(0)$ (eV)	2.907
$S_g^\alpha$	7.8

The temperature behaviour of the Urbach absorption edge in  $\text{Cu}_{5.46}\text{P}_{1.68}\text{S}_{5.06}\text{I}_{0.80}$  thin film is explained by electron-phonon interaction (EPI) that is strong in the film under investigation. The EPI parameters are obtained from the temperature dependence of absorption edge steepness parameter (Fig. 2) using the Mahr formula [13]

$$\sigma(T) = \sigma_0 \cdot \left(\frac{2kT}{\hbar\omega_p}\right) \cdot \tanh\left(\frac{\hbar\omega_p}{2kT}\right), \quad (2)$$

where  $\hbar\omega_p$  is the effective phonon energy in the one-oscillator model describing EPI, and  $\sigma_0$  – parameter related to the EPI constant  $g$  as  $\sigma_0 = (2/3)g^{-1}$  (parameters  $\hbar\omega_p$  and  $\sigma_0$  are given in Table 2). For the  $\text{Cu}_{5.46}\text{P}_{1.68}\text{S}_{5.06}\text{I}_{0.80}$  thin film  $\sigma_0 < 1$ , which is the evidence for strong EPI [14].

It should be noted that, within the range of exponential behaviour of optical absorption for their spectral characterization, one can use the energy position of the exponential absorption edge  $E_g^\alpha$  at a fixed absorption coefficient  $\alpha$ . We used the  $E_g^\alpha$  values taken at  $\alpha = 5 \cdot 10^4 \text{ cm}^{-1}$  for characterization of the absorption edge spectral position (Table 2). The temperature dependences of  $E_g^\alpha$  and the Urbach energy  $E_U$  for  $\text{Cu}_{5.46}\text{P}_{1.68}\text{S}_{5.06}\text{I}_{0.80}$  thin film are presented in Fig. 3 and can be described in the Einstein model by relations [15, 16]

$$E_g^\alpha(T) = E_g^\alpha(0) - S_g^\alpha k\theta_E \left[ \frac{1}{\exp(\theta_E/T) - 1} \right], \quad (3)$$

$$E_U(T) = (E_U)_0 + (E_U)_1 \left[ \frac{1}{\exp(\theta_E/T) - 1} \right], \quad (4)$$

where  $E_g^\alpha(0)$  and  $S_g^\alpha$  are the energy position of absorption edge at 0 K and a dimensionless constant, respectively;  $\theta_E$  is the Einstein temperature, corresponding to the average frequency of phonon excitations in a system of non-coupled oscillators,  $(E_U)_0$  and  $(E_U)_1$  are constants. The obtained  $E_g^\alpha(0)$ ,  $S_g^\alpha$ ,  $\theta_E$ ,  $(E_U)_0$ , and  $(E_U)_1$  parameters for the thin film are given in Table 2, and the temperature dependences of  $E_g^\alpha$  and the Urbach energy  $E_U$  for  $\text{Cu}_{5.46}\text{P}_{1.68}\text{S}_{5.06}\text{I}_{0.80}$  thin film calculated from Eqs. (3) and (4), are shown in Fig. 3 as solid and dashed lines, respectively.

An essential characteristic of the absorption edge spectra of the thin films under investigation is a lengthy Urbach tail, which results in high values of the Urbach energy  $E_U$  (Table 2). In Ref. [17], it was shown that temperature and structural disordering affect Urbach absorption edge shape, i.e. the Urbach energy  $E_U$  is described by the equation

$$E_U = (E_U)_T + (E_U)_X = (E_U)_T + (E_U)_{X,stat} + (E_U)_{X,dyn}, \quad (5)$$

where  $(E_U)_T$  and  $(E_U)_X$  are the contributions of temperature-related and structural disordering to  $E_U$ , respectively;  $(E_U)_{X,stat}$  and  $(E_U)_{X,dyn}$  are the contributions of static structural disordering and dynamic structural disordering to  $(E_U)_X$ , respectively. The static structural disordering  $(E_U)_{X,stat}$  in  $\text{Cu}_6\text{PS}_5\text{I}$  thin film is primarily caused by structural imperfectness due to the high concentration of disordered copper vacancies, and the dynamic structural disordering  $(E_U)_{X,dyn}$  is related to the intense motion of mobile copper ions participating in ion transport and is responsible for the ionic conductivity. The first term in the right-hand side of Eq. (4) represents static structural disordering, and the second one represents temperature-related types of disordering: temperature disordering due to thermal lattice vibrations and dynamic structural disordering due to the presence of mobile ions in the superionic conductor.

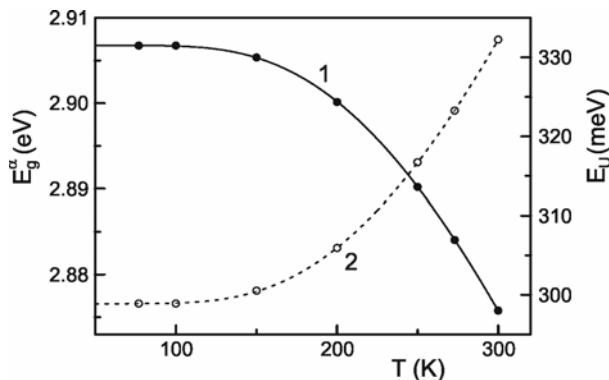


**Fig. 3.** Temperature dependences of the absorption edge energy position  $E_g^\alpha$  ( $\alpha = 5 \cdot 10^4 \text{ cm}^{-1}$ ) (1) and Urbach energy  $E_U$  (2) of the  $\text{Cu}_{5.46}\text{P}_{1.68}\text{S}_{5.06}\text{I}_{0.80}$  thin film.

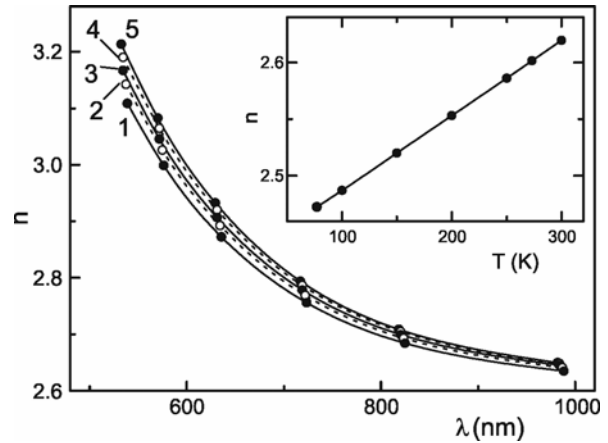


**Fig. 4.** Refractive index dispersions of  $\text{Cu}_{5.46}\text{P}_{1.68}\text{S}_{5.06}\text{I}_{0.80}$  thin film at various temperatures: 77 K (1), 150 (2), 200 (3), 250 (4), and 300 (5). The inset shows the temperature dependence of refractive index.

It is shown that the contribution of static structural disordering into the film Urbach energy equals 90%. Static structural disordering in  $\text{Cu}_{5.46}\text{P}_{1.68}\text{S}_{5.06}\text{I}_{0.80}$  thin film may be additionally increased due to: (1) the absence of long-range order in the atomic arrangement and chemical bond breakdown; (2) lower density of the atomic structure packing related with the presence of pores; (3) the transition from the three-dimensional bulk structure to the two-dimensional planar structure.

The dispersion dependences of the refractive index for the  $\text{Cu}_{5.46}\text{P}_{1.68}\text{S}_{5.06}\text{I}_{0.80}$  thin film was obtained from the interference transmission spectra (Fig. 4). The slight dispersion of the refractive index is observed in the transparency region, while it increases when approaching to the optical absorption edge region. With the temperature increase, the linear increase of refractive index in  $\text{Cu}_{5.46}\text{P}_{1.68}\text{S}_{5.06}\text{I}_{0.80}$  thin film is revealed.

#### 4. Conclusions

$\text{Cu}_6\text{PS}_5\text{I}$ -based thin films are deposited onto silicate glass substrates by using non-reactive radio-frequency magnetron sputtering. When the Cu content increases, a red shift of the optical transmission spectra as well as increase of the total electric conductivity are observed. The spectral dependences of the absorption coefficient and dispersion dependences of the refractive index are derived from the spectrometric studies of interference transmission spectra. A typical Urbach bundle is observed, the temperature behaviour of the Urbach absorption edge in  $\text{Cu}_{5.46}\text{P}_{1.68}\text{S}_{5.06}\text{I}_{0.80}$  thin film is explained by strong electron-phonon interaction. Temperature dependences of the absorption edge energy position and the Urbach energy for  $\text{Cu}_{5.46}\text{P}_{1.68}\text{S}_{5.06}\text{I}_{0.80}$  thin film are well described by the Einstein model. The influence of different type disordering on the Urbach tail for  $\text{Cu}_{5.46}\text{P}_{1.68}\text{S}_{5.06}\text{I}_{0.80}$  thin film has been studied.

### Acknowledgements

Andrii Bendak (contract number 51501903) is strongly grateful to the International Visegrad Fund scholarship for funding the project.

### References

1. W.F. Kuhs, R. Nitsche, K. Scheunemann, Vapour growth and lattice data of new compounds with icosahedral structure of the type  $\text{Cu}_6\text{PS}_5\text{Hal}$  (Hal = Cl, Br, I) // *Mat. Res. Bull.* **11**, p. 1115-1124 (1976).
2. T. Nilges, A. Pfitzner, A structural differentiation of quaternary copper argyrodites: Structure – property relations of high temperature ion conductors // *Z. Kristallogr.* **220**, p. 281-294 (2005).
3. I.P. Studenyak, M. Kranjčec, Gy.Sh. Kovacs, I.D. Desnica, V.V. Panko, V.Yu. Slivka, Influence of compositional disorder on optical absorption processes in  $\text{Cu}_6\text{P}(\text{S}_{1-x}\text{Se}_x)_5\text{I}$  crystals // *J. Mat. Res.* **16**, p.1600-1608 (2001).
4. I.P. Studenyak, M. Kranjčec, M.V. Kurik, Urbach rule and disordering processes in  $\text{Cu}_6\text{P}(\text{S}_{1-x}\text{Se}_x)_5\text{Br}_{1-y}\text{I}_y$  superionic conductors // *J. Phys. Chem. Solids*, **67**, p. 807-817 (2006).
5. A. Gagor, A. Pietraszko, D. Kaynts, Diffusion paths formation for  $\text{Cu}^+$  ions in superionic  $\text{Cu}_6\text{PS}_5\text{I}$  single crystals studied in terms of structural phase transition // *J. Solid State Chem.* **178**, p. 3366-3375 (2005).
6. I.P. Studenyak, V.O. Stefanovich, M. Kranjčec, D.I. Desnica, Yu.M. Azhnyuk, Gy.Sh. Kovacs, V.V. Panko, Raman scattering studies of  $\text{Cu}_6\text{PS}_5\text{Hal}$  (Hal = Cl, Br and I) fast-ion conductors // *Solid State Ionics*, **95**, p. 221-225 (1997).
7. I.P. Studenyak, M. Kranjčec, Gy.Sh. Kovacs, V.V. Panko, D.I. Desnica, A.G. Slivka, P.P. Guranich, The effect of temperature and pressure on the optical absorption edge in  $\text{Cu}_6\text{PS}_5\text{X}$  (X = Cl, Br, I) crystals // *J. Phys. Chem. Solids*, **60**, p. 1897-1904 (1999).
8. Gy.Sh. Kovacs, A.N. Borets, I.P. Studenyak, V.V. Panko, I.I. Rosola, Optic-refractometric relation and refraction index dispersion in  $\text{Cu}_6\text{PS}_5\text{Hal}$  crystals // *Ukr. Fiz. Zhurnal*, **31**, p. 1201-1204 (1986).
9. A.L. Despotuli, A.V. Andreeva, B. Rambabu, Nanoionics of advanced superionic conductors // *Ionics*, **11**, p. 306-314 (2005).
10. I.P. Studenyak, M. Kranjčec, V.Yu. Izai, A.A. Chomolyak, M. Vorohota, V. Matolin, C. Cserhati, S. Kökényesi, Structural and temperature-related disordering studies of  $\text{Cu}_6\text{PS}_5\text{I}$  amorphous thin films // *Thin Solid Films*, **520**, p. 1729-1733 (2012).
11. I.P. Studenyak, M. Kranjčec, A.A. Chomolyak, M. Vorohota, V. Matolin, Optical absorption and refractive properties of superionic conductor  $\text{Cu}_6\text{PS}_5\text{I}$  thin films // *Nanosystems, nanomaterials, nanotechnologies*, **10**, p. 489-496 (2012).
12. F. Urbach, The long-wavelength edge of photographic sensitivity and of the electronic absorption of solids // *Phys. Rev.* **92**, p. 1324-1326 (1953).
13. H. Sumi, A. Sumi, The Urbach-Martienssen rule revisited // *J. Phys. Soc. Japan*, **56**, p. 2211-2220 (1987).
14. M.V. Kurik, Urbach rule (Review) // *phys. status solidi (a)*, **8**, p. 9-30 (1971).
15. M. Beaudoin, A.J.G. DeVries, S.R. Johnson, H. Laman, T. Tiedje, Optical absorption edge of semi-insulating GaAs and InP at high temperatures // *Appl. Phys. Lett.* **70**, p. 3540-3542 (1997).
16. Z. Yang, K.P. Homewood, M.S. Finney, M.A. Harry, K.J. Reeson, Optical absorption study of ion beam synthesized polycrystalline semiconducting  $\text{FeSi}_2$  // *J. Appl. Phys.* **78**, p. 1958-1963 (1995).
17. G.D. Cody, T. Tiedje, B. Abeles, B. Brooks, Y. Goldstein, Disorder and the optical-absorption edge of hydrogenated amorphous silicon // *Phys. Rev. Lett.* **47**, p. 1480-1483 (1981).